Journal of Cardiovascular Magnetic Resonance

Oral presentation

Open Access

Visualization of ablation lesions by dynamic contrast-enhanced (DynCE) MRI

Andriy Shmatukha*[1], Bharathi Sundaram[2], Xiuling Qi[2], Samuel Oduneye[2], Jeffrey Stainsby[1], Graham Wright[2] and Eugene Crystal[2]

Address: [1]General Electric Healthcare, Toronto, ON, Canada and [2]Sunnybrook Health Sciences Centre, Toronto, ON, Canada
* Corresponding author

from 13th Annual SCMR Scientific Sessions
Phoenix, AZ, USA. 21-24 January 2010

Published: 21 January 2010

Journal of Cardiovascular Magnetic Resonance 2010, **12**(Suppl 1):O25 doi:10.1186/1532-429X-12-S1-O25

This abstract is available from: http://jcmr-online.com/content/12/S1/O25

Introduction

Intra-operative lesion visualization is important during ablative cardiac procedures whose success depends on the contiguity and transmurality of the ablation lesions. The usefulness of contrast kinetics analysis for thermal lesion visualization has been already demonstrated [1,2]. However, the method relied on lengthy image acquisition and model-based curve fitting of complete data sets. Delayed enhancement (DE) methods [3-5] required lengthy scan and waiting (after contrast agent, CA, injection) times. Non-enhanced visualization [6] delivered lower lesion-to-background contrasts. We report a novel method for analyzing MRI-apparent contrast uptake dynamics, which allows robust and quick visualization of RF lesions.

Purpose

Identify an approach for rapid and reliable visualization of radiofrequency (RF) ablation lesions suitable for intra-operative usage on combined XMR suites.

Methods

Using clinical EP catheters, 16 RF lesions were created in the Latissimus dorsi muscles of 4 rabbits with power/time settings varying in the range 30-35 Watt/30-45 sec. T1w, T2w, SSFP, DE and Dynamic Contrast-Enhanced (DynCE MR) images of the lesions were acquired 2-3 hours after the ablations. One animal was also imaged 1 week after the ablation.

DynCE images were acquired simultaneously with CA injection using RF-spoiled FGRE. 4-5 slices were imaged in 3:31-6:33 minutes with temporal resolution of 8-19 seconds. 4-10 minutes after CA injection, DE images were acquired using IR-FSPGR.

DynCE images were post-processed on a stand-alone workstation using in-house developed algorithms and software. Cumulative intensity difference (CID) and ratio (CIR) maps, together with their inclination maps, were calculated on each dynamic data set using only the previous and current dynamics. The location, size, and appearance of the lesions, identified on the maps, were compared to currently available imaging standards for lesion visualization [3-6].

Results

Our DynCE analysis algorithms allow reliable differentiation between non-perfused lesion core, hyper-enhanced lesion border and normal tissue in a very short time following CA injection on noisy data sets (Fig. 1), which conventional semi-quantitative DynCE processing methods are not well suited to. CID and CIR maps, together with corresponding inclination maps (Fig. 2), depicted thermal lesions correctly and with satisfactory contrast as compared to the available standards (Fig. 3). Conventional methods are unable to deliver comparable results on the same data sets (Fig. 4).

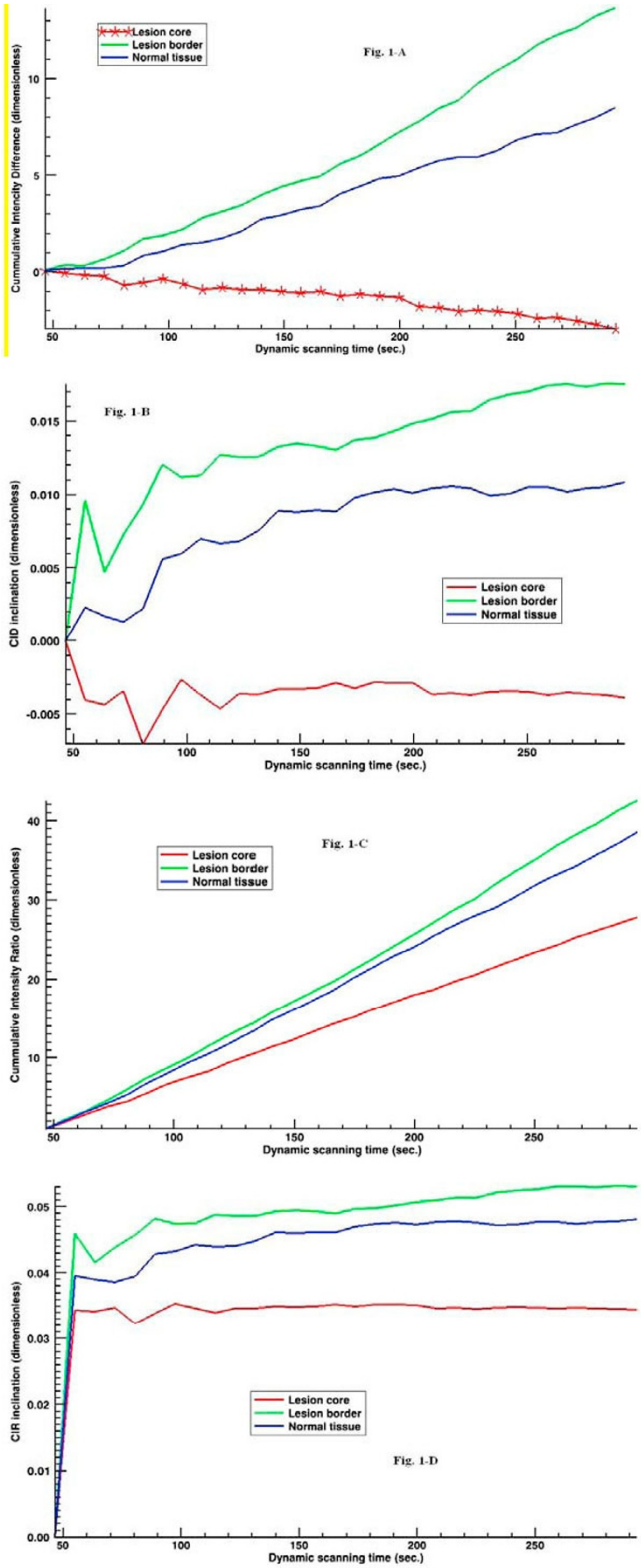

Figure 1

Figure 1
Time course of CID (Fig. 1-A), CIR (Fig. 1-C) and their inclinations (Fig. 1-B and Fig. 1-D correspondingly) for three single pixels chosen inside a lesion, on its border and in healthy tissue. The lesion is marked by the red arrows on the consequent images. The differences between the pixels become apparent as early as 100 sec. after the start of dynamic scanning. Four slices were acquired with the temporal resolution of 8.5 sec.

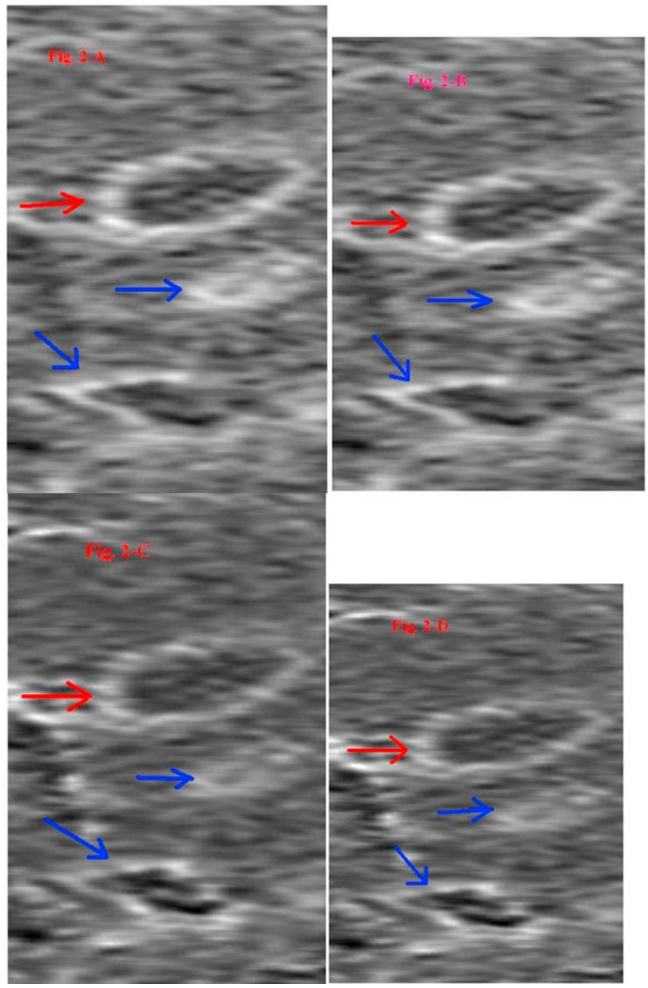

Figure 2
Maps of CID (2-A), its inclination (2-B), CIR (2-C) and its inclinations (2-D). One (of 3) lesions is seen in full cross section (red arrows), and other 2 are partially visible (blue arrows) due to the 2D slice angulation.

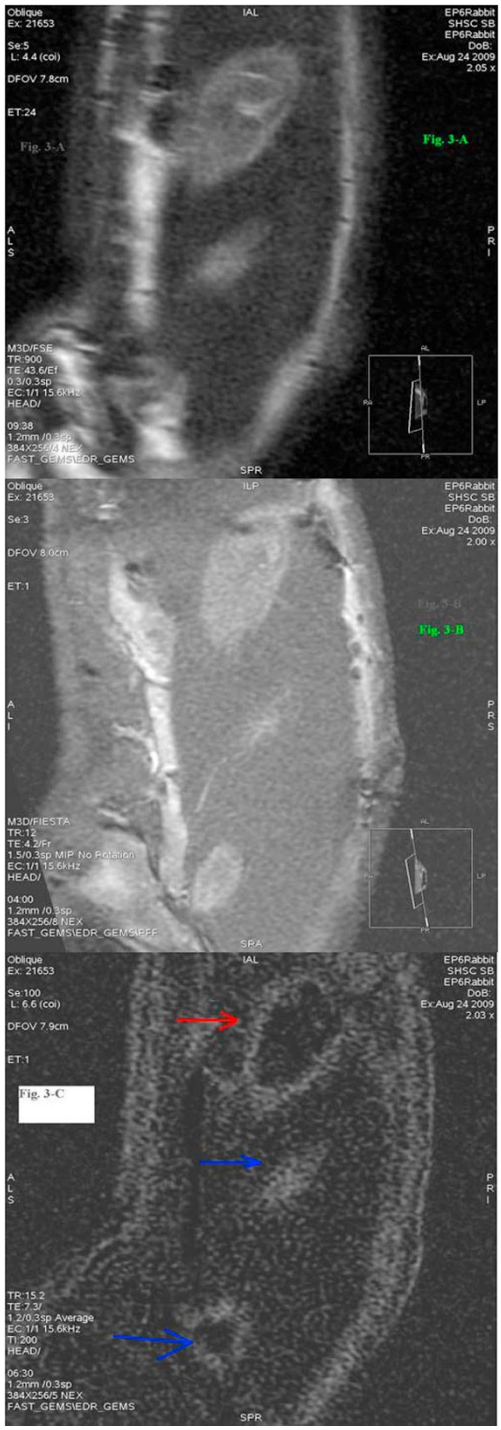

Figure 3
T2w FSE (3-A), SSFP (3-B) and DE IR-FSPGR (3-C) images of the lesions. The exact angulation of the slices used to acquire the DynCE images was difficult to reproduce, so 3D rendering was used to analyze the lesions. The DE IR-FSPGR image was obtained by subtracting a 3D set acquired before CA injection from a similar 3D set acquired ~5 min. after CA injection, and rendering the difference in 3D.

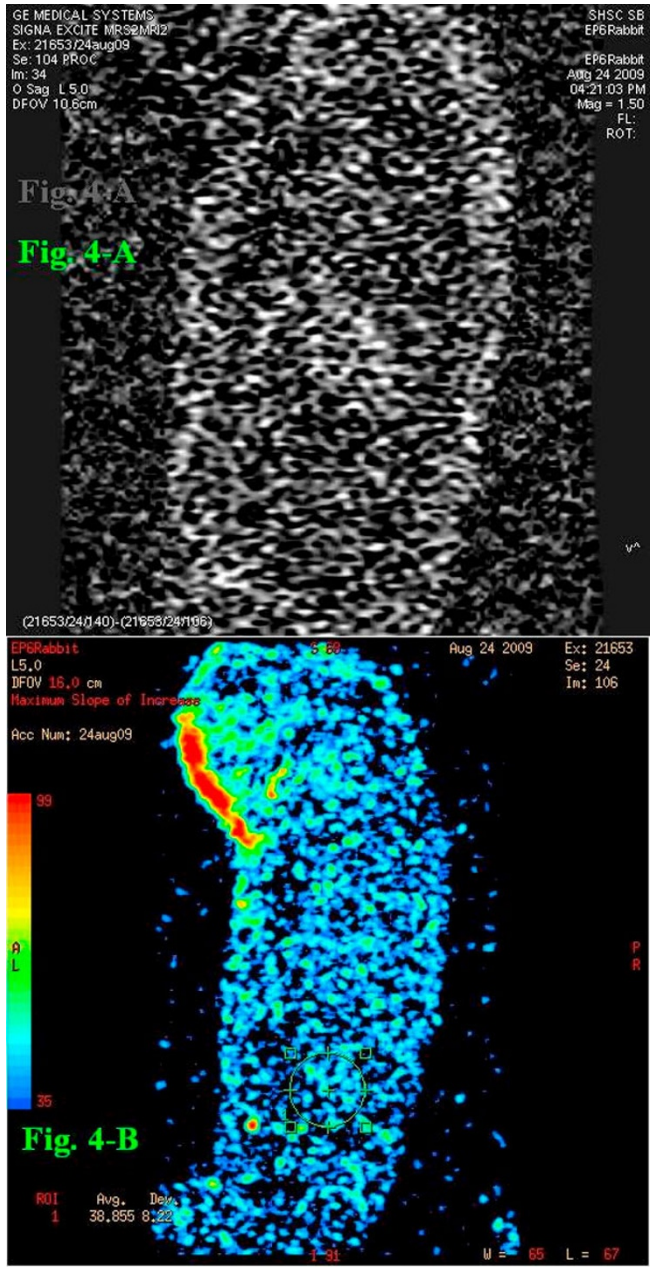

Figure 4
Examples of the conventional CE difference image (4-A), which was obtained by subtracting a pre-contrast baseline from a dynamic CE image, and maximum slope of increase map (4-B) that were calculated after the same amount of time as the maps on Fig 2.

Conclusion

The proposed DynCE analysis algorithms are suitable for rapid intra-operative RF lesion visualization and can be used on combined XMR suites if the images are acquired with proper cardiac and respiratory gating. They could be used for automated thermal lesion detection.

References

1. *J Magn Reson Imaging* 2003, **18:**585-598.
2. *J Magn Reson Imaging* 2004, **19:**329-341.
3. *Med Phys August* 2009, **36(8):**3521-3535.
4. *J Am Coll Cardiol* 2006, **47:**370-378.
5. *Circulation* 2000, **102:**698-705.
6. *HeartRhythm* 2007, **4:**208-214.